Altered ultrastructure of rinderpest virus and its nucleocapsids induced by 5-fluorouracil

Arundhati Ghosh*, R. Nayak* and M. S. Shaila*†

*Department of Microbiology and Cell Biology, †Centre for Genetic Engineering, Indian Institute of Science, Bangalore 560 012, India

The ultrastructure of purified rinderpest virus and intracellular viral nucleocapsids from infected vero cells treated with a subtoxic dose of 5-fluorouracil (5-Fu) (1 μg/ml), has been analysed by transmission electron microscopy, and compared with that of normal virus particle and nucleocapsids. The results reveal dramatic alterations in the structure of both virions and nucleocapsids. The surface glycoprotein projection of virions was not seen or present at a much reduced level. The intracellular nucleocapsids showed pronounced structural changes with respect to size, shape and fine structure. The length of treated nucleocapsids is much smaller as compared to the control. The central hollow core is missing in case of drug-treated nucleocapsid and the herring bone structure is replaced by a 'beads on string' structure. The presence of N protein, which is a major structural component of nucleocapsids was seen in 5-Fu-treated cells, but it was associated with a predominantly diffused form of nucleocapsids as seen by immunoelectron microscopy. We report here the first definitive and visual evidence of altered structure of virions and their nucleocapsids after 5-Fu treatment.

5-FLUOROURACIL (5-Fu) has found extensive use in cancer chemotherapy and is known to inhibit growth of cells by at least three different mechanisms. Fluorouracil is converted into fluorodeoxyuridine monophosphate which inhibits thymidylate synthetase and thereby inhibits DNA synthesis[1,2]. The antimetabolite is incorporated into DNA, leading to fragmentation of DNA[3]. 5-Fu is incorporated into various species of RNA, which has been considered a major reason for the anticancer action of the drug[4–8].

5-Fu has been used as an antiviral agent specially against DNA viruses like the Papilloma[9], herpes and vaccinia viruses[10]. It has been used as a mutagen against animal RNA viruses[11–15] and bacteriophage[16]. The RNA-mediated biological activity of the drug suggests that it can be used as an antiviral agent against RNA viruses. The early work on the antiviral effect of this drug on RNA viruses has been equivocal. On the one hand, it has been shown that 5-Fu did not affect replication of poliovirus[17], while on the other hand, 5-Fu showed marked effect on TMV[18].

We have been studying the RNA-mediated mechanism of action of the drug using rinderpest virus (RPV) as a model system. RPV belongs to the Morbillivirus genus of the Paramyxoviridae family. A number of defined parameters like infectivity, transcription of viral RNA, replication of viral genome and the effect of the drug thereon can be quantitatively evaluated using this system. The genome of this family of viruses contains large stretches of uracil residues at the beginning, end and intergenic region[19]. They make an ideal system to delineate the antiviral mechanism of action of 5-Fu. Our work (to be published elsewhere) shows that 5-Fu treatment reduces the infectivity of the virus and inhibits viral RNA and protein synthesis. This has prompted us to look for the structural basis for the above altered functions of RPV. Therefore the structure of the virus and its nucleocapsids (NC) have been examined through electron microscopy.

Materials and methods

Vero cells (African green monkey kidney cell line) were grown in the presence of various concentrations of 5-Fu and viability tests were done by trypan blue dye exclusion method. Rinderpest virus (attenuated vaccine strain RBOK) was grown in vero cells. The infectivity of the virus particles was measured by $TCID_{50}$ assay[20].

Vero cells were infected with 0.01 $TCID_{50}$ units/cell in the absence or presence of 1 μg/ml of 5-Fu, added at the time of infection. After 72 h, the virus released into the supernatant and cell associated virus released from cell monolayers by freeze-thaw cycles were pooled and clarified by centrifugation at 1000 *g* for 15 min at 4°C. The virus was then pelleted at 100,000 *g* in a Beckman ultracentrifuge using SW28 rotor for one h. The pellet was resuspended in phosphate buffered saline (PBS) and layered over 15% sucrose (w/w), pelleted onto a 65% sucrose cushion in Tris-EDTA (pH 7.5) by centrifugation at 110,000 *g*, in a Beckman SW41 rotor for one h. The opalescent virus band at the 15%–60% sucrose interphase was collected, diluted with PBS and pelleted again at 100,000 *g*. The virus pellet was resuspended in a small volume of PBS and the protein concentration was determined by Lowry's method[21]. The virus samples were further purified by banding on a 15 to 50% (w/w) continuous potassium tartarate gradient by centrifugation at 200,000 *g* in a Beckman SW41

rotor for 18 h. The opalescent virus band was collected, diluted with PBS and pelleted by centrifugation at 110,000 *g* for one h. Protein was estimated again to calculate the final yield. Nucleocapsids were purified from virus-infected cells according to the method of Udem and Cook[22] with a little modification. Infected and drug-treated cell monolayers showing 75–100% spread of cytopathic effects (cpe) were washed with PBS. The cells were scraped using a rubber policeman, washed once with PBS by centrifugation at 2000 *g*. The cell pellet (10^7 cells) was then suspended in hypotonic buffer (10 mM sodium phosphate pH 7.4 and 1 mM PMSF) for 10 min and lysed by the addition of nonidet P-40 to a final concentration of 1% (w/v). Nuclei were removed by centrifugation at 1000 *g* for 2 min. The supernatant was centrifuged at 180,000 *g* in a Ti-50 rotor. Pellet was resuspended in PBS and loaded on a discontinuous CsCl step gradient (1 ml of 40% CsCl w/w, 1.25 ml 30% CsCl, 1.25 ml 20% CsCl, 1 ml of 5% sucrose). Centrifugation was performed using a Beckman SW50 rotor at 210000 *g* for 4 h. The visible band of nucleocapsids was aspirated with a bent pasteur pipette from 30% CsCl region. The nucleocapsids so isolated were washed with PBS by centrifugation at 180000 *g* in a Beckman Ti-50 rotor for 30 min. The final yield from normal and treated cells was quantified.

Electron microscopic studies

Aliquots of virus and nucleocapsids (equal µg quantity of protein from normal and treated) were placed on copper grids covered with formvar film. After two min. of adsorption at room temperature, the samples were negatively stained with 2% potassium phosphotungstate for five min. Specimens were examined in a Jeol 100 CxII electron microscope at 80 kV.

Nucleocapsids were measured from EM negatives at 95× magnification with the aid of Wild–Heerbrugg M8 zoom stereomicroscope. About 34 of normal NCs and 15 of treated NCs were measured. A small scale graticule was used for measuring the length.

Immunoelectron microscopy

Nucleocapsids were adsorbed to formvar-coated grids, and the grids were rinsed with Tris buffered saline (500 nm NaCl, 25 mM Tris-HCl, pH 7.6). The grids were floated on drops of 3% gelatin in TBS to minimize non-specific binding of antibodies on grid surface[23]. The grids were then floated on the solution of primary antibody (rabbit anti N polyclonal antibody, diluted 25-fold with TBS containing 1% gelatin), incubated for 1 h at 37°C, rinsed and floated on a 1 : 20 diluted solution of goat–antirabbit antibody conjugated with 5 nm gold particles (Bioclin, GAR-LM, UK). After 1 h of incubation, the grids were thoroughly rinsed with TBS, negatively stained with 2% potassium phosphotungstate and observed under the electron microscope. Controls were used in which primary antibody was omitted.

Results

The production of infective particles was checked at a range of fluorouracil concentration starting from 0.1 µg/ml to 10 µg/ml. The objective was to determine a drug concentration well below the CD_{50} value of the drug for vero cells (CD_{50} 20 µg/ml) which is inhibitory to production of infective particles. There was a 99% reduction in infectivity at drug concentration of 1 µg/ml. There was no further reduction in infectivity till 7 µg/ml of drug concentration. Since 1 µg/ml drug concentration is not toxic to vero cells and is well below the CD_{50} dose, we used this dose for the rest of the experiments. The drug can affect both the host cells as well as the virus. Therefore it is essential to avoid the secondary effect of the host cell toxicity on virus production.

Electron microscopic examination of the virus revealed that virions from untreated cells have a typical pleiomorphic range of particle size of 200–650 nm, with majority of the particles coming within the range of 200–300 nm. Similar results have been reported by Plowright[24], wherein most particles were in the range of 120–300 nm while the size of some particles ranged up to 750 nm. Kesari[25] has reported the size of rinderpest virus particles to be in the range of 100–200 nm. The minor differences reported in these studies are not surprising considering the pleiomorphic nature of the virus. Figure 1 *a* shows a virion on which the external glycoprotein spikes are clearly visible. The negative staining has also penetrated the interior, revealing the nucleocapsids packed inside the particle. In sharp contrast, virions from 5-Fu-treated cells exhibited a particle size range of 50–200 nm, with some larger particles with up to 400 nm diameter, smaller size virions being preponderent. In addition, the morphological features of RPV recovered from 5-Fu-treated cells were drastically different, in that neither the glycoprotein containing surface spikes nor the characteristic, loosely packed coils of the nucleocapsid could be seen (Figure 1 *b*). Taken together, these results suggest that at least the virus assembly process was affected adversely in the 5-Fu-treated cells.

Since 5-Fu was expected to get incorporated into viral genomic RNA, which might in turn affect the defined nucleocapsid structure of RPV, it is easier to visualize the structural alteration brought about by drug effect. We examined NCs isolated from both untreated and 5-Fu-treated cells. The electron micrographs of the NC from untreated and 5-Fu-treated cells are shown in

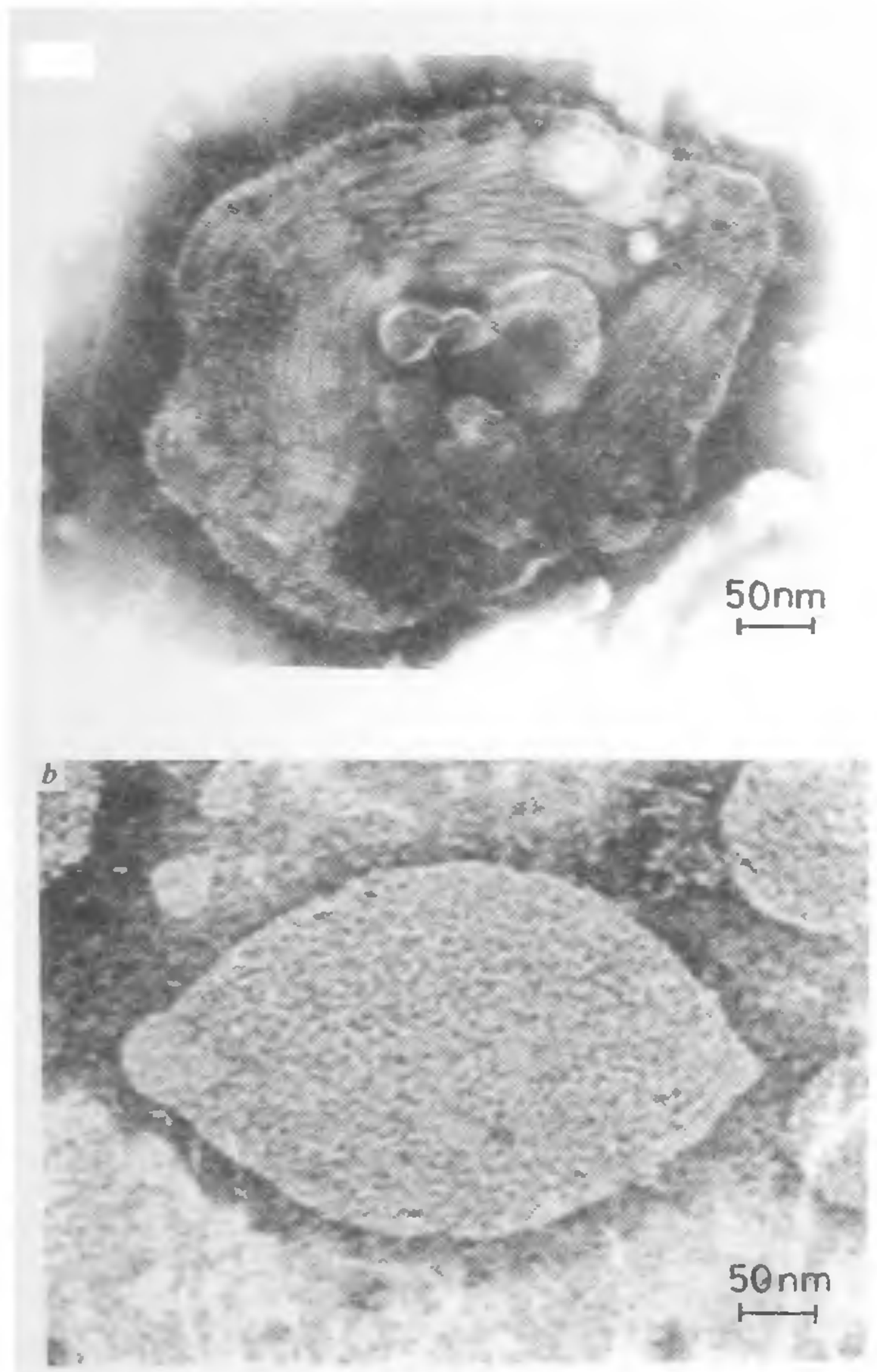

Figure 1. Electron micrograph of purified rinderpest virus (*a*) and purified virus grown on 5-Fu-treated vero cells (*b*) negatively stained with 2% phosphotungstate. Magnification 17400×.

Figure 2*a* and *b*, and their corresponding enlarged sections in Figure 2*c* and *d* respectively. NC from untreated infected cells appeared as relatively long, rigid, linear molecules with typical herring-bone appearance (Figure 2*a*), closely resembling NCs from measles virus[26]. In contrast, NC from 5-Fu-treated cells showed striking morphological difference. The NC preparation showed a 'beads on string' appearance and they were short fragments of varying lengths (Figure 2*b*). The central hollow core was not discernable. Examination of the Figures 2*a–d* as well as the data presented in Table 1 demonstrate the nature of differences seen between the NC preparations. The length of NCs in case of normal ranged from 1010 nm to 1290 nm with average of 1144 ± 62 nm (mean length ± standard deviation of the mean), whereas the treated ones showed a particle size ranging from 189 nm to 220 nm with an average of 195 ± 26 nm. The average length of NC preparation from drug-treated cells was found to be nearly six times smaller than normal. The number of helical turns in case of normal NCs was found to be 197 ± 19, whereas in case of treated, 31 ± 12. There was a linear relationship between length and number of helical turns in both normal and treated NCs. The diameter of standard NC is 18 ± 0.28 nm, the diameter of central hollow core being 5.5 ± 0.12 nm and the pitch is 5.7 ± 0.17 nm, which falls within the range of diameter and pitch as reported by Plowright[24], in RPV (the diameter of the particle is 17.5 nm, pitch is 5–6 nm). The diameter of the NC-strands from 5-Fu-treated cells was 8.7 ± 0.22 nm, which is less than half the value (18 nm) of normal nucleocapsids. The typical 'herring bone' morphology of normal nucleocapsids can be contrasted to a 'beads on string' appearance of NC preparations recovered from 5-Fu-treated cells. We rationalize that this change is due to an apparent absence of a central hollow core in the drug-induced abnormal NCs. Not only is the absence of this core visually apparent (Figure 2*d*), but also the geometry of both NCs suggest this possibility. For instance, we could measure from Figure 2*c* that the normal NC has a diameter of 18 nm with a core of 5.5 nm whereas the diameter of 5-Fu induced abnormal NC measured 8.7 nm (Figure 2*d*). Our results show further that the pitch of the abnormal nucleocapsid (6.2 ± 0.11 nm) was affected only marginally, retaining nearly 92% of its normal value. Helix angle and subunit angles were calculated according to the method described by Lund *et al.*[26] and found to be 9° and 60° in case of normal and 0° and 40° in case of treated respectively. Taken together, we conclude that 5-Fu has a deleterious effect on the NC assembly/organization and this may be a possible mode of antiviral action of this drug.

Immuno electron microscopic observation of normal NC (Figure 3*a*) revealed that the N protein was distributed over the entire length of NC. This is expected since N (nucleocapsid protein) has been shown to cover the entire length of genomic RNA of Paramyxoviruses[19]. NC from treated cells also revealed the presence of N protein (Figure 3*b*) although the lengths of such NC were shortened. This demonstrates that the altered structures produced in the cells due to 5-Fu treatment are virus-specific and are not aberrant cellular components. Moreover, this experiment shows that although N protein is synthesized in 5-Fu-treated cells, they are unable to organize the nucleocapsid in a normal manner presumably due to structural changes in the RNA molecule as a result of 5-Fu incorporation.

Discussion

5-Fu has been reported to alter the structure of various RNA species. No data are available on the altered

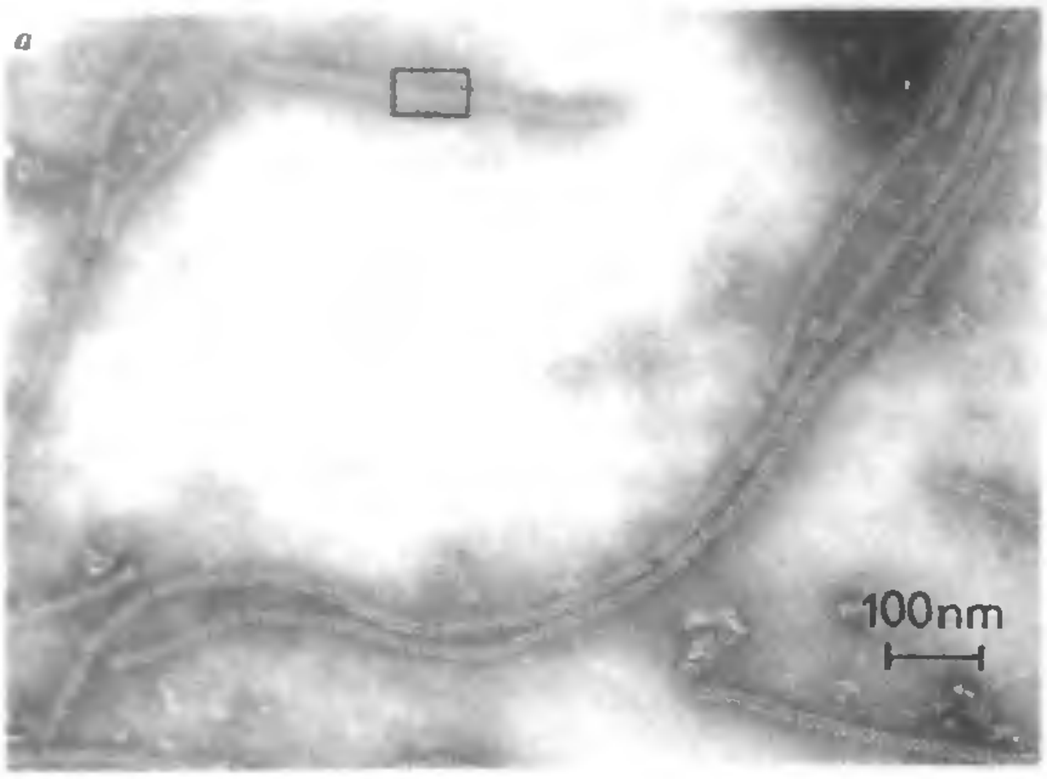

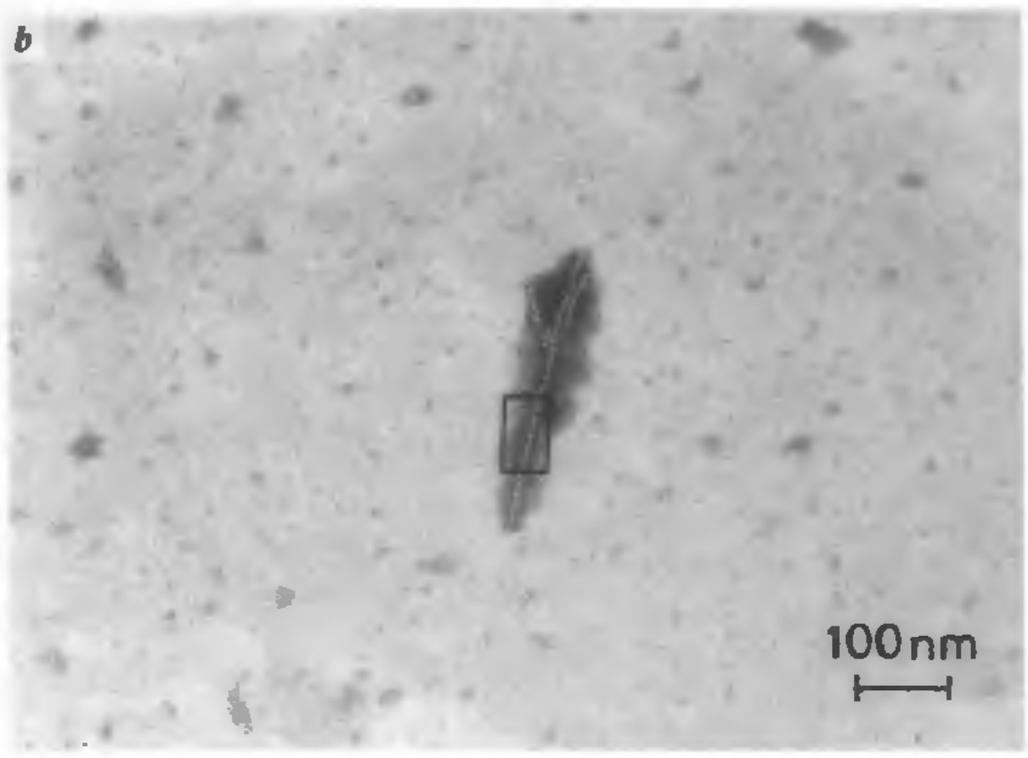

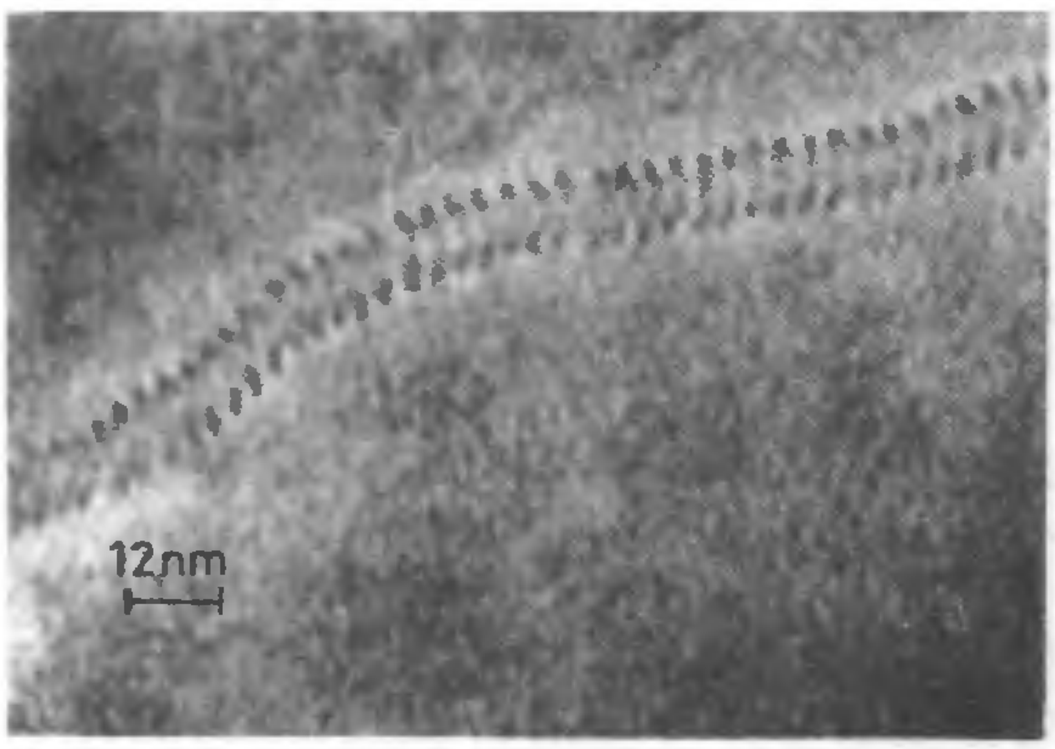

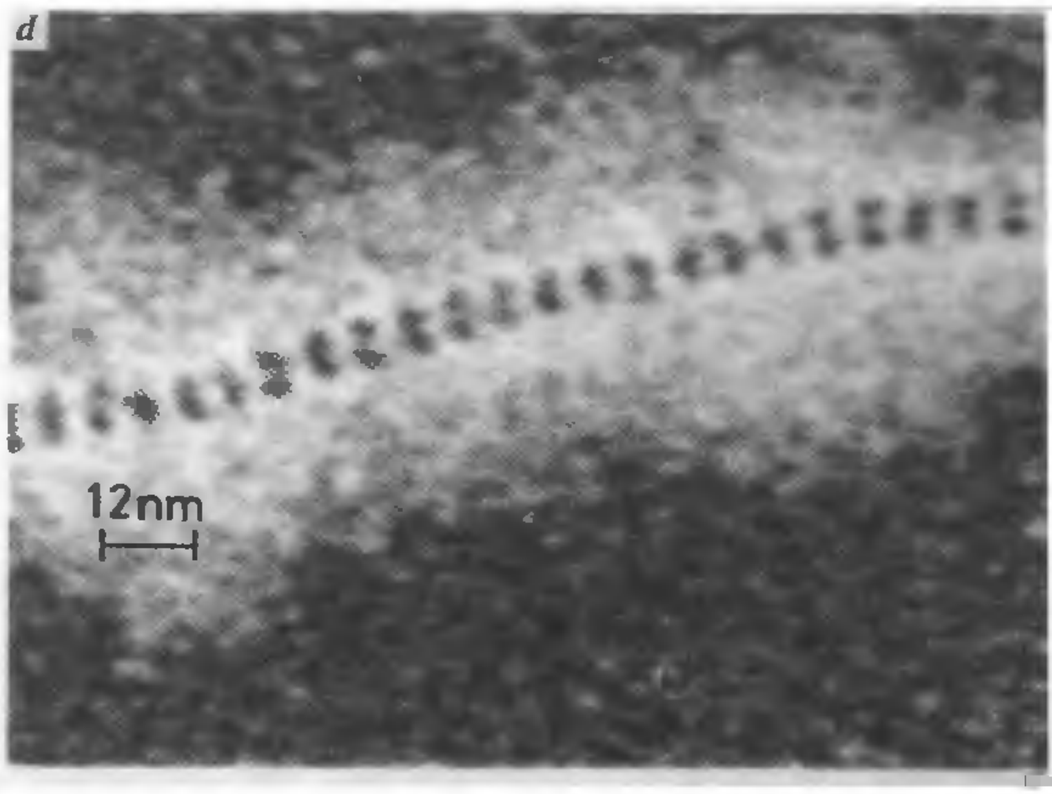

Figure 2. Electron micrograph of purified nucleocapsids from *a*, rinderpest virus infected vero cells and *b*, 5-Fu-treated infected cells Magnification 106400×; *c* and *d*, Portions of *a* and *b* magnified further (8×).

Table 1. Physical characteristics of nucleocapsid of rinderpest virus from normal and 5-Fu-treated vero cells

Parameters	Normal nucleocapsids	5-Fu- treated nucleocapsids
Length	1144 ± 62 nm	195 ± 26
No. of helical turns	197 ± 19	31 ± 12
Pitch	5 70 ± 0.17	6.20 ± 0 11
Ext. diameter	18 ± 0 28 nm	8.70 ± 0 22
Diameter of inner hollowcore	5 50 ± 0.12	–
Subunit angle	60°	40°
Helix angle	9°	0°

structure of either viral RNA or subviral particles (nucleocapsid complex) even though 5-Fu has been used as a mutagen[12, 14] to produce attenuated virus as candidate vaccine. We provide here the first definitive and visual evidence of altered structure of virions and their nucleocapsids after 5-Fu treatment.

The treated virions observed under the electron microscopy are different from those of normal virion. These are smaller in size and the surface glycoprotein projections are scanty or absent. The nucleocapsids present inside the particles are not closely packed. The altered virion structure is perhaps reflected in the reduced infectivity of the virus (99% reduction in the infectivity of the virus as measured by $TCID_{50}$ assay, data not shown). It would be interesting to delineate the key steps in the virus replication cycle which abolishes the infectivity.

Our data show clearly and unambiguously that 5-Fu induces structural alterations in the newly formed RPV and in their NCs at very low doses, the most striking feature being the loss of herring bone structure of the nucleocapsids which is replaced by a 'beads on string structure' as noted previously. In independent experiments we have confirmed that 5-Fu is incorporated into virion-specific RNAs (data not shown) and the structural

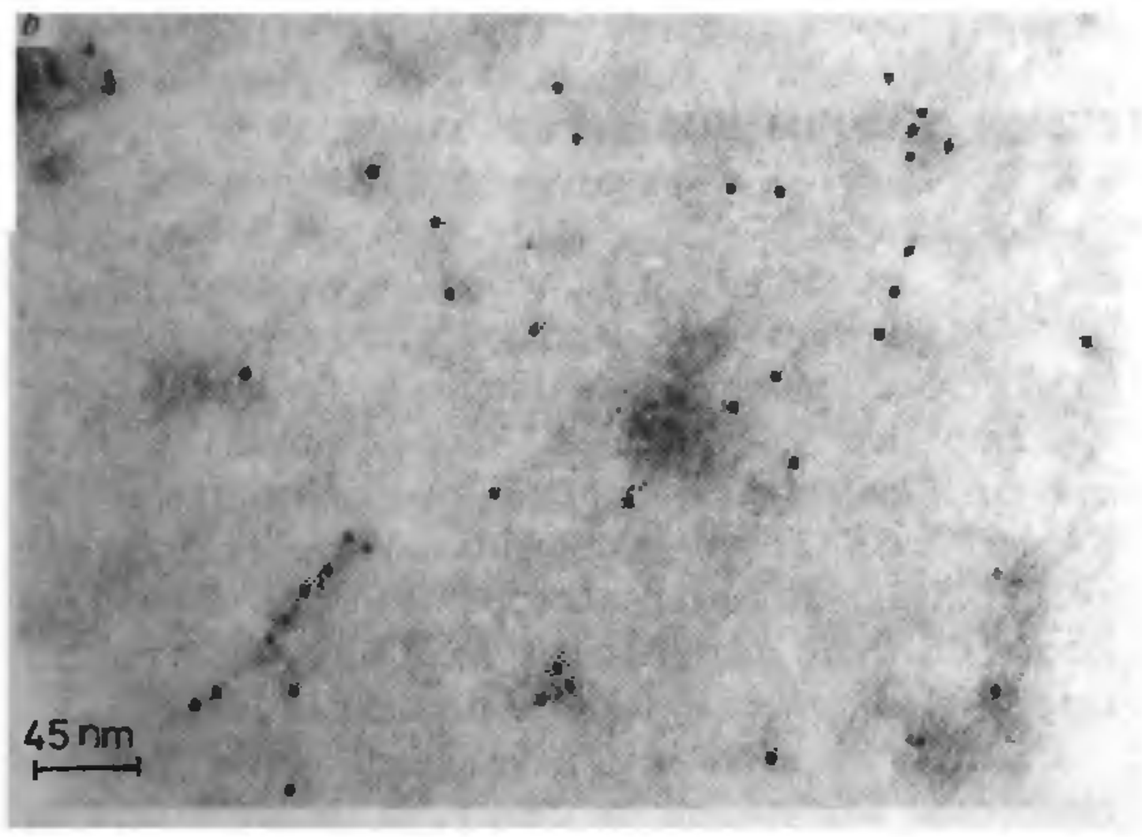

Figure 3. Immuno electron micrograph of nucleocapsids from *a*, rinderpest virus infected vero cells and *b*, 5-Fu-treated infected cells Magnification 220000×.

alterations reported here may be a direct result of 5-Fu substitutions in RNA. We note, however, that our data do not exclude indirect effects contributing to these structural changes such as: an altered metabolic state of vero cells upon drug treatment, although no toxic effect of 5-Fu on vero cells treated with similar dose of 5-Fu was discernible in control experiments. Parameters of structural alterations observed with nucleocapsids recovered from 5-Fu-treated cells suggest that the central core may be missing from them. The exact biochemical reason for this alteration is not yet known. Various possibilities are that the N-protein synthesized in the drug-treated cells may be limiting or that N-protein fails to participate in the nucleocapsid assembly in a normal manner due to 5-Fu incorporation into viral RNAs or both. As noted previously, relatively large stretches of uracil residues are found in the intergenic regions as well as at 5′ and 3′ ends of paramyxo virus RNA. Substitution of these with a fluoro-analogue might render RNA molecules to become fragile at the substitution sites, thereby accounting for a reduction in the average size of these NCs. The fragility of RNA due to 5-Fu substitution has been reported for tRNA[27]. Additional experiments will be required to understand the molecular basis of such morphological changes induced by 5-Fu.

Structurally altered NCs also have been seen in persistent infection of measles[28] and mumps viruses[29]. There are interesting similarities and differences, e.g. for mumps virus, where the pitch increases as in treated RPV NC, but the external diameter also increases, unlike that of RPV NC here. However, this is the first observation of structural alteration of nucleocapsids after treatment with a drug.

In conclusion, our finding that a small and pharmacologically relevant dose of the drug can alter the structure of an RNA virus and its nucleocapsid and has potent antiviral effect, may pave the way for evaluating the efficacy of the drug against other RNA viruses which are causative agents of a large number of human and animal diseases.

1. Heidelberger, C., *Cancer Res*, 1970, **30**, 1549–1569.
2. Hartman, K U. and Heidelberger, C., *J. Biol. Chem.*, 1961, **236**, 3006–3013
3 Lonn, U and Lonn, S., *Cancer Res*, 1984, **44**, 3414–3418.
4 Spiegelman, S, Sawyer, R., Nayak, R, Ritzi, E, Stolfi, R. and Martin, D, *Proc Natl Acad Sci USA*, 1980, **77** 4966–4970.
5 Doong, D L. and Dolnick, B. J, *J. Biol. Chem.*, 1988, **263**, 4467–4473.
6 Herrick, D and Kufe, D W, *Mol Pharmacol.*, 1984, **26**, 135–140.
7. Cohen, N B. and Glazer, R. I., *Mol Pharmacol*, 1984, **27**, 308–313.
8 Wilkinson, D. S. and Crumley, J, *J Biol. Chem.*, 1977, **252**, 1051–1056
9 Brillhart, J. R, *Indiana Med*, 1990, **83** 652–656.
10. Dragun, M, Rada, B, Norotny, H and Beranck, J, *Acta Virol Praha*, 1990, **34**, 321–329.
11 Tolson, N. D., Chartton, K M, Steward, R. B, Casey, G. A., Webster, N. A. and Mackenzie, K, *Can. J. Vet Res.*, 1990, **54**, 178–183.
12 Takehara, K., Min, M. K., Battles, J K, Sugiyama, K., Emergy, V. C, Dalrymple, J N and Bishop, D. H, *Virology*, 1989, **169**, 452–457
13. Chui, L. W., Vainionpae, R, Marusyk, R, Salmi, A. and Norrby, E J, *Gen Virol*, 1986, **67**, 253–261.
14 Caplan, H., Peters, L. J. and Bishop, D H J., *Gen Virol.*, 1985, **66**, 2271–2277.
15. Shimura, Y. and Nathans, D., *Biochem. Biophys. Res. Commun.*, 1964, **16**, 116–120.
16 Cooper, P D., *Virology*, 1964, **22**, 186–192.
17. Muniyon, N. and Salzman, N. P, *Virology*, 1962, **18**, 95–101
18 Gordon, M. P. and Stachelin, M, *Biochem. Biophys Acta*, 1959, **36**, 351–361.
19. Galinski, M. S and Wechester, S L., in *The Paramyxoviruses* (ed Kingsbury, D N), Plenum, New York, 1991, pp 66–68.
20 Reed, L H. and Muench, H, *Am J Hyg*, 1938, **37**, 493
21. Lowry, O H, Rosebrough, N J, Farr, A L and Randall, R J, *J Biol Chem*, 1951, **193**, 265 275

22 Udem, S A and Cook, R A, *J. Virol*, 1984, **49**, 57–65.
23 Portner, A and Murti, K G, *Virology*, 1986, **150**, 469–478
24 Plowright, W, *Virol Monogr*, 1962, **3**, 29–30.
25 Kesari, K. V, Ph D Thesis, Indian Institute of Science, Bangalore, 1985
26 Lund, G A, Tyrrel, D L J, Bradley, R D and Scrabin, D. G, *J Gen Virol*, 1984, **65**, 1535–1542.
27. Kumar, A M and Nayak, R, in *Contemporary Themes in Biochemistry* (eds. Kon, O, *et al*), ICSU Press, 1986, pp. 182–183
28 Andzhaparidze, O. G., Chaplygina, N. M, Bogomolova, N. N, Lottie, N D, Koptyaeva, I. B and Boriskin, Yu. S., *Arch. Virol.*, 1987, **95**, 17–28
29 Andzhaparidze, O G, Boriskin, Yu S., Bogomolova, N. N and Lottie, N. D, *Arch Virol*, 1983, **75**, 283–289.

ACKNOWLEDGEMENTS. We thank R. Rangeswaran for his expert assistance in electron microscopy. We also thank Bhuvaneshwari of Molecular Biophysics Unit for helping with the use of stereomicroscope This research was supported by a grant under the Molecular Virology Programme from the Department of Biotechnology, Government of India

Received 20 April 1994, revised accepted 11 July 1994

A study on the comparison of CSAMT and MT data

I. B. Ramaprasada Rao, Ram Raj Mathur and S. Srinivas

Centre of Exploration Geophysics, Osmania University, Hyderabad 500 007, India

Analysis of Controlled Source Audio Frequency Magneto Telluric (CSAMT) data is conventionally carried out using Cagniard resistivity under far field conditions. However, the near field response, which cannot be avoided in the field operations, differs considerably from the far field response. The discrepancy has been recognized the world over. In India the potential of CSAMT has not been exploited in its entirety. To bridge this gap on the Indian scene, a beginning has been made by studying the far field–near field discrepancies. The near field response in CSAMT for Vertical Magnetic Dipole (VMD) and Horizontal Electric Dipole (HED) is computed for homogeneous and two layer media. The critical frequency below which the near field conditions validity is studied, and the correction factor to make near field data look like far field data over a homogeneous medium discussed.

THE Controlled Source Audio-Frequency Magneto-telluric method (CSAMT)[1,2] is a frequency domain electromagnetic sounding technique with a fixed grounded electric dipole or horizontal loop (or a vertical magnetic dipole) as signal source. Stronger and stable signal, time invariance of the primary field polarization and its selectability confer a marked advantage for CSAMT over natural source methods (MT and AMT).

While two perpendicular horizontal components of electric and magnetic fields (E_x and H_y) are measured in scalar CSAMT, E_x, H_y, H_x and H_z components are measured in vector CSAMT. Usually five components (namely E_x, E_y, H_x, H_y and H_z) with two source polarizations are measured in Tensor CSAMT.

CSAMT results have been reported over sulphide targets[3], over massive sulphide body in Japan[4], over lead/zinc/silver deposit in Alaska[5], over uranium and sulphide/graphite targets[4], over base metals in Finland[6–8]. CSAMT measurements have been carried out by Uchida *et al.*[9] over a copper/lead/zinc deposit in Japan. CSAMT measurements have also been proved successful in the search for gold deposits in Japan[10].

CSAMT measurements have been carried out for geothermal exploration in USA[12], in Japan[4,13] and in Hawaii[14]. In petroleum exploration, CSAMT has been used for structural mapping[4,15–18].

CSAMT method proved effective in the investigations for groundwater quality[19–23], for structural analysis in mine planning[24], detecting voids in underground mines[25], mapping burn fronts in underground coal gasification and coal mine fires[24,26]. However, practically no study has been reported from India.

Far field and near field

Usually, if the transmitter receiver separation $\mathbf{r} \ll \delta$ and the induction number $|kr| \ll 1$ (where $|k| = (\sigma\mu\omega)^{1/2}$ is the wave number of quasistatic case) it is known as the 'near field' zone. On the other hand if $\mathbf{r} \gg \delta$, $|kr| \gg 1$ it is known as 'far field' zone.

The theory for the MT, AMT, AFMAG and VLF case is well-formulated since the source independence of the EM field is assumed[27]. However, in CSAMT as the receiver–transmitter separation becomes less than 3 skin depths (skin depth, $\delta = (2/\sigma\mu\omega)^{1/2}$ for quasistatic case) at low frequencies, the field becomes 'near field' rather